Rapid Impact Testing for Quantitative Assessment of Large Populations of Bridges

Yun Zhou, John Prader, John DeVitis, Adrienne Deal, Jian Zhang, Franklin Moon*, A. Emin Aktan
Drexel University, Drexel Intelligent Infrastructure Institute. 3141 Chestnut St, Philadelphia, PA, 19104

ABSTRACT

Although the widely acknowledged shortcomings of visual inspection have fueled significant advances in the areas of non-destructive evaluation and structural health monitoring (SHM) over the last several decades, the actual practice of bridge assessment has remained largely unchanged. The authors believe the lack of adoption, especially of SHM technologies, is related to the 'single structure' scenarios that drive most research. To overcome this, the authors have developed a concept for a rapid single-input, multiple-output (SIMO) impact testing device that will be capable of capturing modal parameters and estimating flexibility/deflection basins of common highway bridges during routine inspections. The device is composed of a trailer-mounted impact source (capable of delivering a 50 kip impact) and retractable sensor arms, and will be controlled by an automated data acquisition, processing and modal parameter estimation software. The research presented in this paper covers (a) the theoretical basis for SISO, SIMO and MIMO impact testing to estimate flexibility, (b) proof of concept numerical studies using a finite element model, and (c) a pilot implementation on an operating highway bridge. Results indicate that the proposed approach can estimate modal flexibility within a few percent of static flexibility; however, the estimated modal flexibility matrix is only reliable for the substructures associated with the various SIMO tests. To overcome this shortcoming, a modal 'stitching' approach for substructure integration to estimate the full Eigen vector matrix is developed, and preliminary results of these methods are also presented.

Keywords: Bridge assessment, structure identification, modal flexibility, impact testing, substructure integration

1. INTRODUCTION

Bridges are the most critical components within the highway transportation system. The American Society of Civil Engineers (ASCE) [1] reports that the average annual public investment into transportation infrastructure is approximately $60 billion with 85% going to the expansion or maintenance of the highway system. In another report [2], an estimated $2.2 trillion is needed to bring the country's overall infrastructure up to good working order, while $150 billion per year is especially staggering. According to the FHWA [3], over 33% of the 604,485 bridges in the U.S. were built over 50 years ago, among which 43% are rated either structurally deficient or functionally obsolete. Lack of funding notwithstanding, it is becoming increasingly clear that the current approaches to bridge assessment and decision-making are unsustainable. Of particular concern is the exclusive reliance on visual inspection, which has been shown to have significant variability and is inherently qualitative in nature (which makes comparison between bridges and inspectors challenging).

In contrast, the paradigm of structural identification (St-Id) [4] permits quantitative characterizations of constructed facilities and their loading environments at various performance levels and resolutions. Visual approaches used in condition and structural assessment and for designing interventions in the case of deterioration, damage and other performance problems such as excessive vibrations often prove unreliable. On the other hand, significant technology expertise and associated costs in addition to large user costs may discourage condition assessment based on St-Id especially when controlled load testing is used. Such drawbacks of cost and disruption of service ultimately discourage widespread applications of St-Id.

The research reported here aims at leveraging modal analysis through transient excitation (impact) for measuring modal flexibility of bridge superstructures as a quantitative measure of condition and changes in condition. Past research by the writers [5-7] revealed that flexibility and changes in flexibility may serve as an excellent measure of bridge condition and performance. Theoretically, a single reference accelerometer at the driving or impact point would be adequate for extracting all the frequencies and mode shapes that have non-zero amplitudes at that reference based on the single input-single output (SISO) modal analysis method. While this is theoretically possible, the SISO approach does not permit the distinction of real poles from spurious poles and is unable to reliably distinguish between pairs of modes that are inherent to axisymmetric structures. As a result, the writers are exploring the use of a series of single input-multiple output (SIMO) impact tests at selected points to extract valuable quantitative information about bridge flexibility. The advantage of this approach is that a single, self-contained vehicle could be used to carry out such tests, and that it conceivably would require only minor traffic slow-downs on individual lanes of the bridge.

In this paper, the requisite theory is summarized and the proposed methodology is demonstrated through both analysis and experiment. A numerical simulation utilizing a simple plate structure is designed to test the feasibility of SIMO testing coupled with the proposed substructure integration technique. In addition, an impact test was conducted on a real structure. The measured input from the device coupled with the resultant acceleration is used to construct frequency response functions (FRF). From the FRF, modal flexibility at the impact point was estimated by synthesizing FRFs from estimated modal parameters and picking the FRF magnitude at 0 Hz in SISO, SIMO and MIMO cases. An FE model of the single span is created and the extracted modal data from the global MIMO test is used to calibrate the FE model. The calibrated FE model is used as a baseline to evaluate the accuracy of estimated modal flexibility at the impact point. At last, a successful substructure integration method is applied for further validation of the methodology.

2. GSA SYSTEM CONCEPT

The scenario that is envisioned for SIMO applications to bridge superstructures is leveraging a trailer equipped with an impact device pulled by a vehicle along a lane or the centerline of a bridge. The impact device will apply an impact while collecting data via a telescoping reference frame with sensors mounted under the trailer (Figure1).The Global Structure Assessment (GSA) system will be a mobile, autonomous system capable of delivering controlled impacts (comparable to typical truck axle weight) and capturing the resulting free vibration response through a fixed array of sensors. The GSA system and the requirements for rapid deployment will not allow a fixed array of sensors to be employed for the 'best practice' multiple input- multiple output (MIMO) application. The result is that the GSA system will provide a series of independently obtained SIMO tests as it traverses a bridge, with each test delivering an impact and capturing the response of the structure through an array of sensors in the vicinity of the impact. While each of these tests may be processed independently to obtain local flexibility coefficients, it may also be possible to artificially stitch such tests together and process them in an integrated manner to obtain more complete flexibility information.

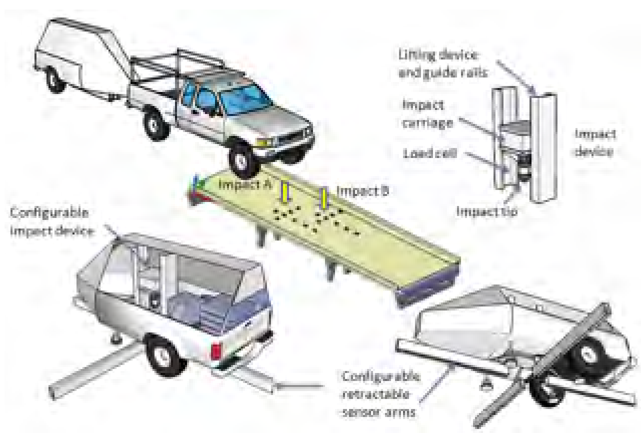

Figure 1. Conceptual diagram of the GSA system

3. MODAL FLEXIBILITY

The concept of flexibility was first introduced by Maxwell in 1864, and the flexibility can be described as the displacements results from the application of a unit force/moment. Modal flexibility, which refers to the estimated static flexibility extracted from modal test results, has been shown to be an accurate approach if sufficient modes are chosen, and this method was first introduced by Clough and Penzien in 1975 [8]. Modal flexibility has been proposed as a reliable signature reflecting the existing condition of a bridge by Raghavendrachar in 1992 [7] and it can also be used to validate modal test results. There are two different approaches for extracting modal flexibility, which require: (1) the extraction of mass normalized mode shapes and modal frequencies, and (2) the identification of a synthesized FRF matrix. These two methods are equivalent and can be used interchangeably.

3.1 Modal flexibility calculation based on unit modal mass (UMM) normalized mode shapes

This method's success depends on the accuracy of the mass normalized mode shapes obtained from an impact test. The transformation of natural frequencies and mode shapes to a unit load flexibility matrix is given by the following expressions:

$$f = [\Phi][\Omega][\Phi]^T \tag{1}$$

Where each entry in the flexibility matrix is given by,

$$f_{i,j} = \sum_{k=1}^{m} \frac{\phi^k(i)\phi^k(j)}{\omega_k^2} \tag{2}$$

Where, f = flexibility matrix; $[\Phi]$ = a matrix of unit modal mass mode shapes matrix (scaled modes); $[\Omega]$ is a diagonal matrix containing the reciprocal of the square of natural frequencies in ascending order; f_{ij} is static displacement of the i-th point resulting from a unit load at the j-th point; ω_i is the i-th circular frequency (radian/second); $\phi^k(i)$ is the modal vector coefficient at the i-th measurement point of the k-th mass-normalized mode. Extracting true mass normalized mode shapes can be difficult since the mass matrix of the structure can have significant errors due to assumptions made in the construction of the modal model.

3.2 Identification FRF matrix at $\omega = 0$ using modal parameter

Utilizing one of a number of available modal parameter estimation algorithms [10], a frequency response function between point p and q can be written in partial fraction form,

$$H_{pq}(\omega) = \sum_{r=1}^{m} \left[\frac{(A_{pq})_r}{j\omega - \lambda_r} + \frac{(A_{pq}^*)_r}{j\omega - \lambda_r^*} \right] \tag{3}$$

The residue term A_{pqr} can be expressed as $(A_{pq})_r = (\psi_{pr}\psi_{qr})/(M_A)_r$, and evaluating H_{pq} at ω=0 for DOF p and q for modes r leads to the modal flexibility matrix. Assuming $Q_{A_r} = 1/M_{Ar}$, and substituting the previous expressions results in:

$$H_{pq}(\omega) = \sum_{r=1}^{m} \left[\frac{\psi_{pr}\psi_{qr}}{M_{A_r}(-\lambda_r)} + \frac{\psi_{pr}^*\psi_{qr}^*}{M_{A_r}^*(-\lambda_r^*)} \right] = \sum_{r=1}^{m} \left[\frac{Q_{A_r}\psi_{pr}\psi_{qr}}{(-\lambda_r)} + \frac{Q_{A_r}^*\psi_{pr}^*\psi_{qr}^*}{(-\lambda_r^*)} \right] \tag{4}$$

Where, $H_{pq}(\omega)$ = FRF at point p due to input at point q; A_{pqr} = residue for mode r; ω = frequency variable; λ_r = r-th complex eigenvalue; ψ_{pq} = mode shape coefficient between point p and q for the r-th mode; M_{Ar} = modal scaling for the r-th mode. This flexibility matrix is an approximation of a real flexibility matrix because of the finite number of modes that can be obtained from modal testing.

3.3 Consistency of Modal Flexibility Methods

While the approaches may appear distinct, in reality these two modal flexibility calculation methods are consistent. If the structure is a proportionally damped system, the modal vectors can be assumed to be real normal modes, therefore the conjugate of a modal vector is the same as the modal vector as shown in Eq. (5),

$$\psi_{pr} = \psi_{pr}^* \tag{5}$$

In Eq.(4), assuming the modal vectors are mass normalized modal vectors, the FRF equation can be rewritten as,

$$H_{pq}(\omega)=\sum_{r=1}^{m}\left[\frac{Q_t\phi_{pr}\phi_{qr}}{(-\lambda_r)}+\frac{Q^*{}_t\phi^*_{pr}\phi^*_{qr}}{(-\lambda^*_r)}\right] \tag{6}$$

In proportionally damped structures, Q_t is related to modal mass and modal frequency by [11],

$$Q_t=\frac{1}{2j\omega_t M_t} \tag{7}$$

Here $M_T=1$ since it is a mass normalized case, if Eq. (4) equals Eq. (6),

$$Q_{A_r}\psi_{pr}\psi_{qr}=Q_t\phi_{pr}\phi_{qr} \tag{8}$$

In modal analysis, Q_{A_r}, ψ_{pr} and ψ_{pr} are known parameters which can directly be extracted from the modal analysis method, and Q_t can be calculated by Eq.(7), if p=q, the response location is also the input location and is known as the driving point. Eq. (8) then can be written as Eq.(9),

$$Q_{A_r}\psi_{pr}\psi_{pr}=Q_t\phi_{pr}\phi_{pr} \tag{9}$$

The mass normalized mode shape coefficient at point p can be easily extracted as shown in Eq. (10),

$$\phi_{pr}=\sqrt{2j\omega_r Q_{A_r}}\cdot\psi_{pr} \tag{10}$$

Then by substituting Eq. (10) into Eq.(8), the remaining mode shape coefficients for the r-th mode can be obtained as shown in Eq. (11),

$$\phi_{qr}=Q_{A_r}\psi_{pr}\psi_{qr}/Q_t\phi_{pr} \tag{11}$$

By using this method, the mass normalized mode shapes can also be deduced, which build a bridge between the former two modal flexibility calculation methods, and it is the theoretical basis for the GSA system substructure integration.

4. NUMERICAL EXPERIMENT

A numerical study was carried out on a simple plate structure as shown in Figure 2 (a). This structure was segmented into a 13 by 4 grid where the nodal points denoted potential impact and sensor locations. To simulate the impact, a time history obtained from a past bridge test performed by the Drexel Team was used, and the response time histories at various grid nodal points were used as the sensor output. The data (input and output time histories), obtained through SISO and various combinations of SIMO testing, was then processed to extract modal parameters and compute modal flexibility using the Poly-reference Time Domain algorithm. The resulting modal flexibility was then compared with the static flexibility of the model to assess to what degree the specific testing approach was reliable. This process is illustrated schematically in Figure 2 (b) for SISO testing of point 29.

The approach of the integration of individual tests without common sensors presents a problem which is illustrated by Figure 3(a) that precludes the estimation of the complete flexibility matrix. To overcome this, a method has been developed that (1) extracts the mass normalized mode shapes for each part of the substructures directly from the residues, scaling factors and pole information produced by modal analysis, and (2) then selects the phase information using heuristics and stitches the modes together (as they have a uniform scaling). It is expected that for the vast majority of bridge types the heuristics required to identify phase information can be captured and automated. When this stitching process is complete the mode shapes are expanded to include all of the measurement points on the bridge and thus the full modal flexibility matrix can be computed using classic modal flexibility approaches.

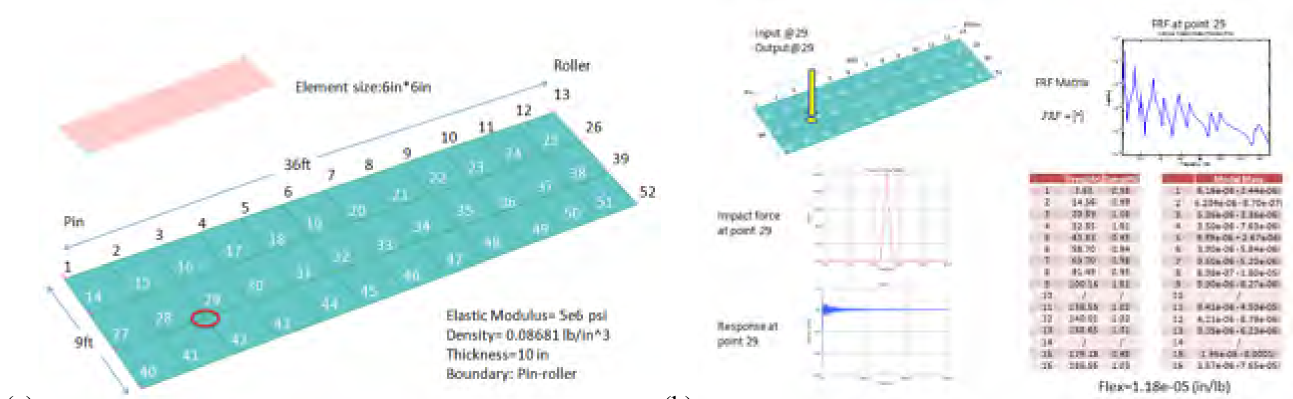

(a) (b)

Figure 2. (a)Numerical model used to assess SISO and SIMO testing approaches (b) Schematic illustrating the simulated testing, data processing, modal parameter estimation and flexibility calculation for SISO testing

To verify the reliability of the substructure integration method, a representative test was performed on this simple plate structure with known flexibility. As seen in Figure 3(b), a SIMO impact test was performed at DOF 29, and anther SIMO impact test was performed at DOF 36, with each impact test including an array of response locations. Using the proposed substructure integration method, the resulting analytical flexibility matrix approximates the known ground truth flexibility matrix with a maximum error of 2%. In this simulation, it has to be emphasized that the impact point should not coincide with the nodal point of the first few modes since these modes contribute significantly to modal flexibility and if they are not well excited their estimation will contain significant errors. The phase information should also be carefully considered when assembling the two substructures in order to correctly piece together the two independent tests. The numerical simulation in this case is conducted in the absence of sensor noise, and the reliability of this method has to be further validated on a real structure where sensor noise and other uncertainties are present.

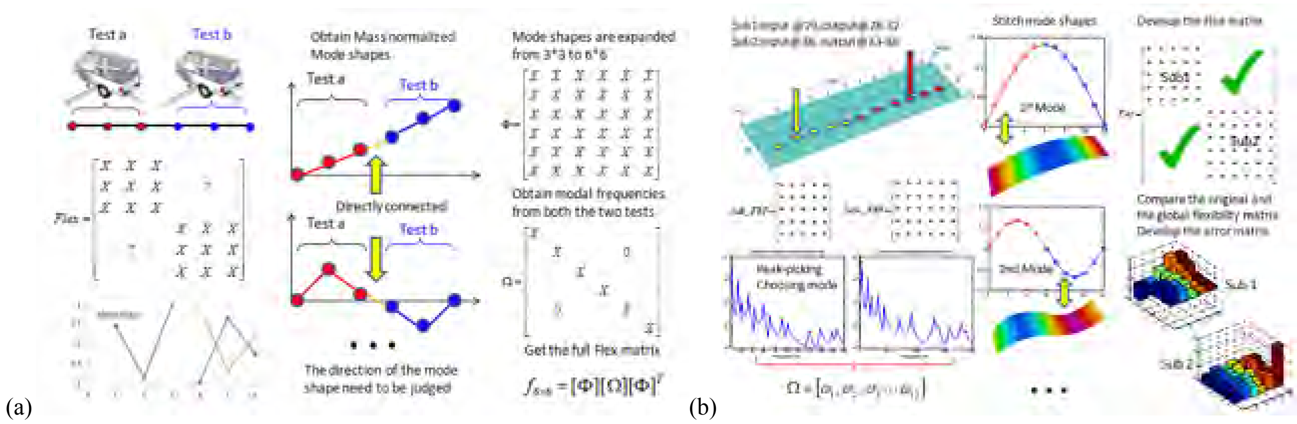

(a) (b)

Figure 3. (a) Schematic illustrating how to stitch two substructures together to integrate the complete modal flexibility matrix (b) Schematic illustrating the substructure integration strategy for simple plate

5. SUBSTRUCTURE MODAL TEST ON THE PENNSAUKEN CREEK BRIDGE

Recently the authors finished a series of modal impact tests on the Pennsauken Creek (PC) Bridge in Palmyra, NJ (Figure 4). The goals of this study were to (1) establish the actual characteristics of various impact sources and free decay responses, (2) examine the suitability of the response for the computation of modal flexibility, and (3) validate the possibility of the SISO and SIMO test procedures and the proposed substructure integration methodology. The PC Bridge is a three span simply-supported steel stringer structure that is representative of the most common bridge type found throughout the U.S. It consists of three spans, each approximately 51 ft. and carries four lanes of traffic in each direction. It has a roadway width of 42 ft. from curb to curb, and concrete sidewalks are present on each side of the bridge with widths of 3 ft. 6 in. Each span consists of a reinforced concrete deck on seven simply supported rolled steel

I-beams with partial-length welded bottom flange cover plates spaced at 7 ft. 2 in. The substructure was composed of reinforced concrete abutments and hammerhead type piers. The bridge deck, sidewalk, parapets and bridge railing were replaced in 2004. The test segment of the bridge consisted of one half of a single span. Traffic control allowed the two lanes included in the test segment to be blocked from traffic, while allowing traffic to proceed on the other two lanes.

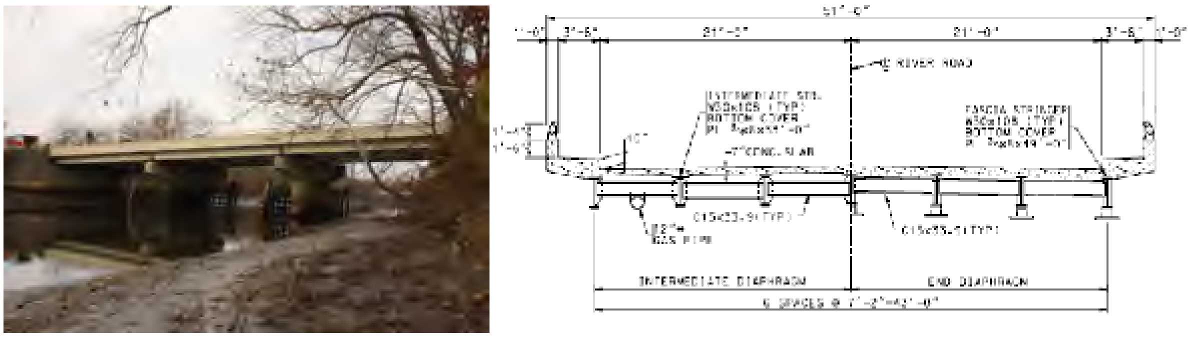

Figure 4. (a) Photograph and (b) Transverse section of the Pennsauken Bridge

5.1 Hammer impact test on the Pennsauken Creek Bridge

Impact excitation is a simple, rapid, and effective way to excite a structure in order to establish the system's FRFs. The local impact test was conducted by using 3 different impact devices. The southbound lanes of the 1st span of the bridge were selected for the impact test by traffic control. Three different impact sources were used including a Swedish drop hammer (rented from The Modal Shop), a drop hammer manufactured in-house at Drexel University, and an instrumented sledge hammer purchased from PCB Piezoelectronics. In this paper, only the data obtained using the Drexel drop hammer is presented (Figure 5(a)).

(a) 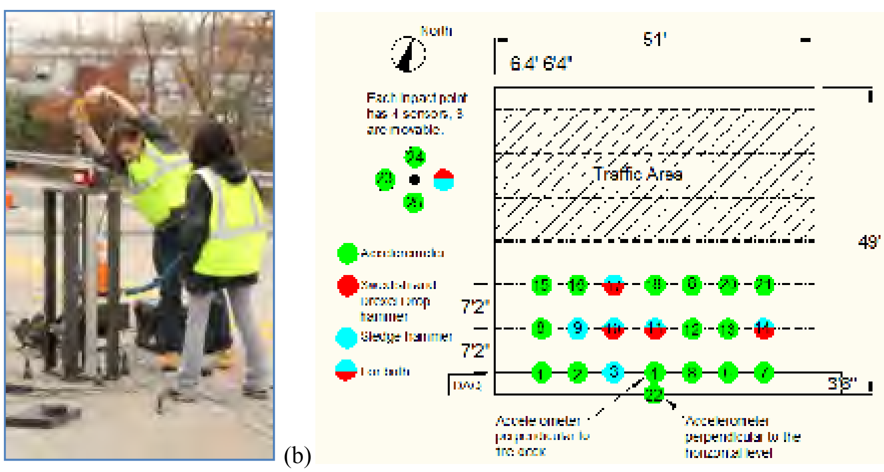 (b)

Figure 5. (a) Photograph of application of Drexel drop hammer on the PC Bridge (b) Dynamic instrumentation layout

In this test, a dynamic signal acquisition module (National Instruments NI9234) with a reconfigurable control and acquisition system (CompactRIO) was used to collect the dynamic data. The ModalView software developed by ABSignal Inc. was utilized for signal processing, frequency analysis and modal analysis. After careful calibration, 25 PCB 393A-03 accelerometers were installed on the top surface of the deck. The sensor layout, which consisted of 21 accelerometers, was designed to ensure that a relatively dense and regular distribution of responses were captured spatially (Figure 5(b)). Three additional sensors were roved around with the impact device to capture the acceleration at the driving point by using various averaging techniques. Points 10, 11, 14 and 17 were selected as the impact locations. The impact tests were conducted between traffic to avoid introducing extraneous sources of excitation.

5.2 Signal processing and modal analysis

The impact signal is a transient deterministic signal which is formed by applying an impulse to a system that lasts for a very small fraction of the total sampling period. The width, height and shape of the pulse time-history determine the usable spectrum of the impact. The sampling frequency for the PC test was set at 826 Hz. The typical impact forces and accelerations at point 10 produced by the Drexel drop hammer are shown in Figure 6 (a)-(b). The Drexel drop hammer had a force level of approximately 18 kips which induced a peak bridge response of roughly 2.05g. As seen in this figure, there were several impulses due to the multiple impacts caused by the rebound of the falling mass, which made the analysis process more difficult.

The raw time histories were preprocessed by adding the rectangular and exponential windows to eliminate the effects of leakage. The windowed time histories are then transformed into auto and cross power spectra using a 16,384 point FFT. The FRFs were estimated using the H1 method and analyzed further using the CMIF modal analysis method to extract the poles, residues and scaling factors , which can be utilized for calculation of modal flexibility as presented in Eq.(4). Auto power spectra for the different impact sources are shown in Figure 6(c). Typically a 20dB drop-off in the spectrum magnitude from 0Hz is taken as the acceptable frequency range based on past tests of constructed systems. As seen from Figure 6(c), the Drexel drop hammer provides a wide useful frequency range at about 170Hz.

(a)

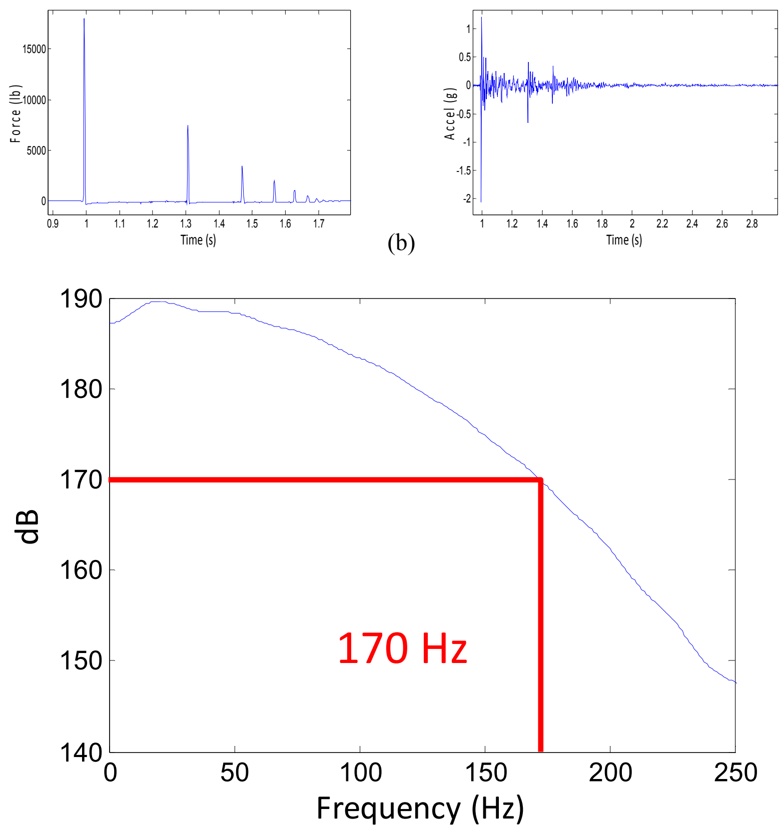

(c)

Figure 6. Drexel drop hammer impact test signal analysis at point 10 (a) Force history signal (b) Acceleration time history signal (c) Force spectrum analysis

5.3 SISO, SIMO and MIMO modal analysis

The GSA system will provide a series of independently obtained SIMO tests as it traverses a bridge, with each test delivering an impact and capturing the response of the structure through an array of sensors in the vicinity of the impact. In this paper, four scenarios of the modal flexibility analysis were conducted to simulate the GSA working status. Four typical scenarios are designed including SISO, SIMO, MIMO, and global cases which are shown in Figure 7. All four scenarios are used to develop the modal flexibility coefficient at point 10 for comparative purposes.

The identified modal flexibility coefficients of point 10 for different cases are listed in Table 1. The flexibility coefficients were estimated consistently between 2.32e-6 in/lb and 2.39e-6 in/lb. This is somewhat surprising since the impact mass for this device rebounds and causes multiple impacts, which violates the underlying assumption of modal testing. This was likely due to the relatively large response that was induced by this impact source which allowed the bridge responses to be captured in a very reliable and accurate manner. To mitigate the multiple impact issues, two approaches were employed. The first approach used the first impact only and windowed the response down before the second impact occurred. This essentially added a significant amount of numerical damping that was later subtracted out of the identified damping coefficient. The second approach processed the entire time window using classical approaches and ignored the fact that multiple impacts occurred. While both approaches produced repeatable results, the second approach is presented in this paper.

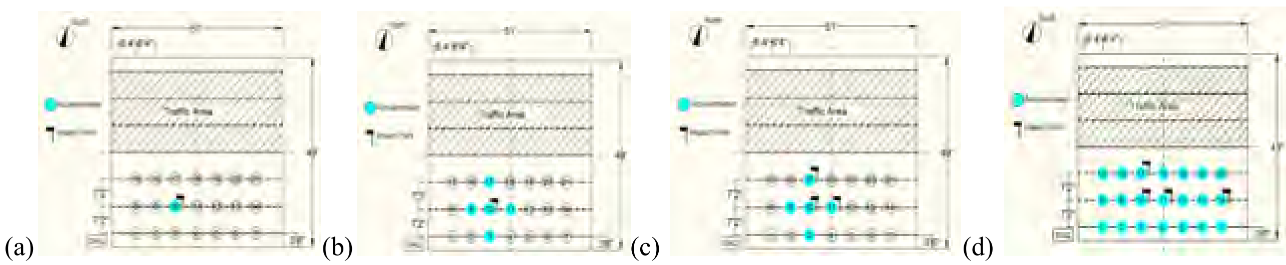

Fig. 7 Illustration of 4 scenarios (a) SISO analysis (b) SIMO analysis (c) MIMO analysis (d) Global analysis

Table 1 Modal flexibility coefficient at point 10 in different cases by CMIF method (Unit: in/lb)

	Global	SISO (local)	SIMO(local)	MIMO(local)
Drexel drop hammer	2.39e-6	2.32e-6	2.33e-6	2.37e-6

5.4 Finite element model validation

After modal flexibility has been obtained, the next challenge is to evaluate the reliability of each modal coefficient shown in Table 1. Ideally, the modal flexibility coefficients would be compared to the static flexibility measured during a truck load test to assess their overall accuracy, but in the envisioned application of the GSA system, time/cost requirements limit the application of the truck load test on the bridge.

In the case of the PC Bridge, a truck load test was not conducted. Without the static test, an a priori FE model was developed to provide a reference for the comparison of modal flexibility (Figure 8). The center line model, which was regarded as the 'best practice' in modeling, was built in Sap2000 software for the tested span. Beam elements were used to model the steel stringers, diaphragms, and parapets while shell elements were used to model the deck and sidewalks. To connect the different structural elements, tunable link elements were used. The model is comprised of 741 beam elements, 2016 shell elements, and 356 link elements. The boundary conditions were modeled with spring elements so the model could be tuned by altering the stiffness of the boundary conditions to calibrate the model output to the measured experimental responses. The vertical slope of the bridge surface as well as the slope to the crown of the roadway were both simulated by the model. The physical parameters of the steel and concrete in the model were chosen from the values documented in the engineering drawings. To ensure the model was a reasonable representation of the structure, one set of boundary conditions (denoted spring-spring) were updated to match the experimental mode shapes. This was carried out by computing the first nine analytical modes (Figure 9) and comparing them with the first nine measured modes (Figure 10).

Along with physical properties of the different bridge components, the boundary conditions are generally considered to have significant influence on the modal parameters of the FE model. Therefore, four different boundary conditions were modeled including pin-pin, pin-roller, fixed-fixed and spring-spring. The first 3 cases are typically used in a-priori FE models and the spring-spring boundary condition was added in order to calibrate the model using the measured modes. To extract the static flexibility coefficients a unit load was applied at point 10 and the resulting displacements corresponded to the flexibility coefficient (Table 2). The most realistic boundary conditions (pin-roller and spring-spring) both generated similar flexibility coefficients and these were well within 5% of those produced using the Drexel drop hammer in all cases (Table 1). While this approach to evaluating the accuracy of the modal flexibility estimates is admittedly not as convincing as a static truck load test, it does provide a very promising independent correlation with the impact tests.

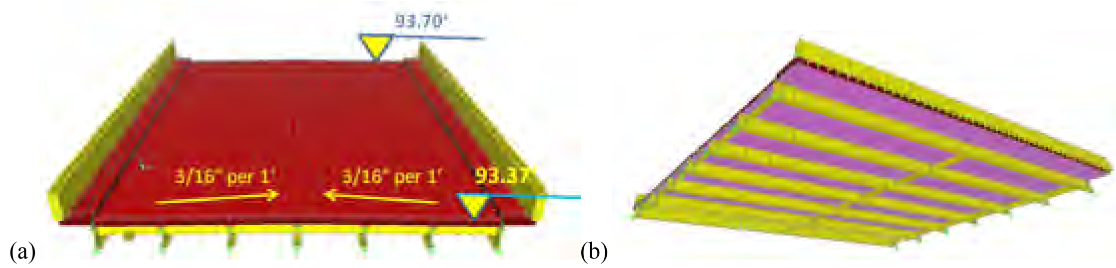

Figure 8. Finite element model for the 1st span of PC bridge (a) Top view (b) Bottom view

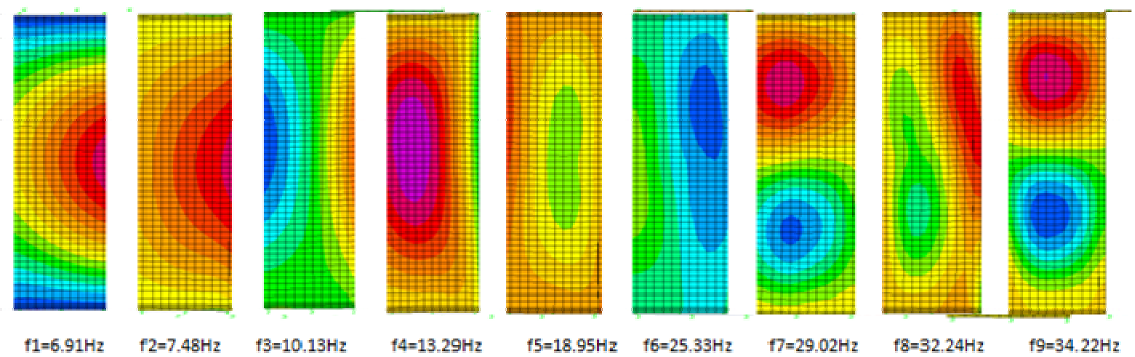

Figure 9. Calculated first 9 modes after preliminary calibration

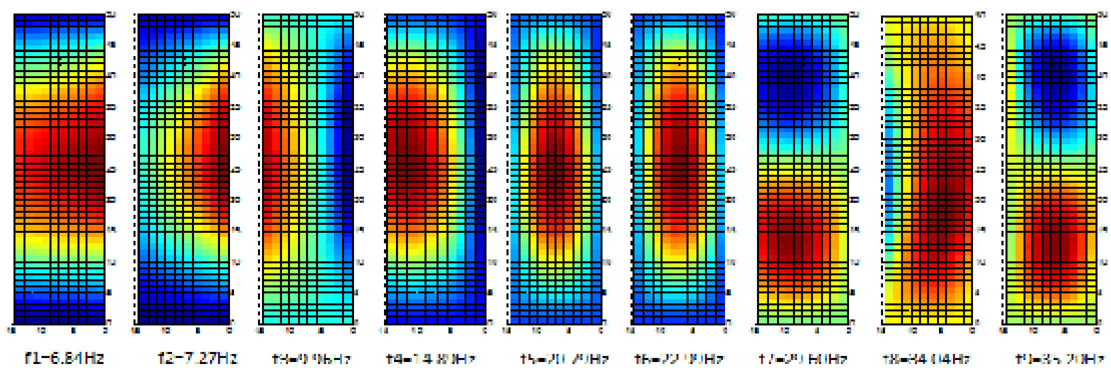

Figure 10. Measured first 9 modes in global test by Drexel drop hammer

Table 2. Static flexibility coefficient at point 10 in different boundary conditions (unit: in/lb)

	Pin-Roller	Pin-Pin	Fix-Fix	Spring-Spring
Static flexibility	2.29e-6	1.35e-6	1.24e-6	2.28e-6

5.6 Substructure integration

After confirming the successful identification of the modal flexibility coefficient at point 10, the proposed substructure integration procedure was employed to stitch together two independent SIMO tests. As seen in Fig. 11(a), two substructure tests were performed at point 10 and point 14, each surrounded with a subset of sensors to measure the response of each substructure. Therefore, two SIMO substructure analyses were conducted to extract the local modal flexibility. The first 9 modes were selected using Peak Picking from the CMIF singular value plot, shown in Figure

11(b), (c), obtained from the CMIF algorithm. The global modes are then assembled as shown in Figure 12. It is shown that the natural frequencies of the two substructures are similar and only vary by a maximum of 2%. The majority of the mass normalized mode shapes can be constructed by simply connecting the two substructures. The one exception is the 5th identified mode which exhibits a dip between the two shapes at the interface. This erroneous shape may be caused by non-coherent excitation (traffic) during one test or errors in the signal processing.

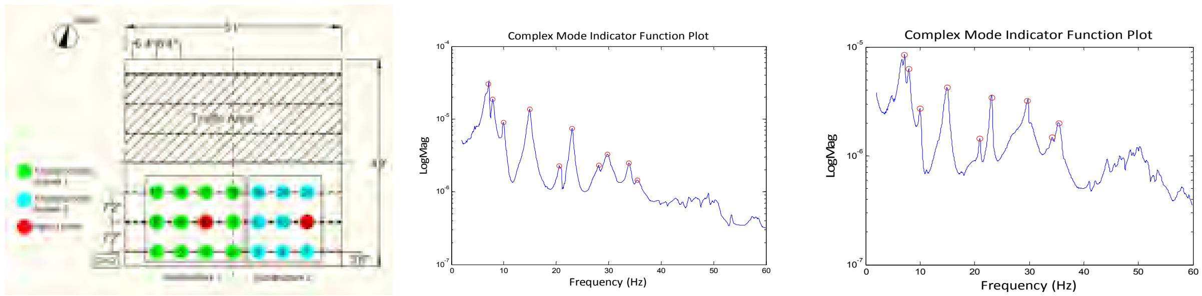

(a) (b) (c)

Figure 11. (a) Substructure integration experiment on the PC Bridge (b) Peak-Picking in CMIF SV figure for substructure 1 and (c) Peak-Picking in CMIF SV figure for substructure 2

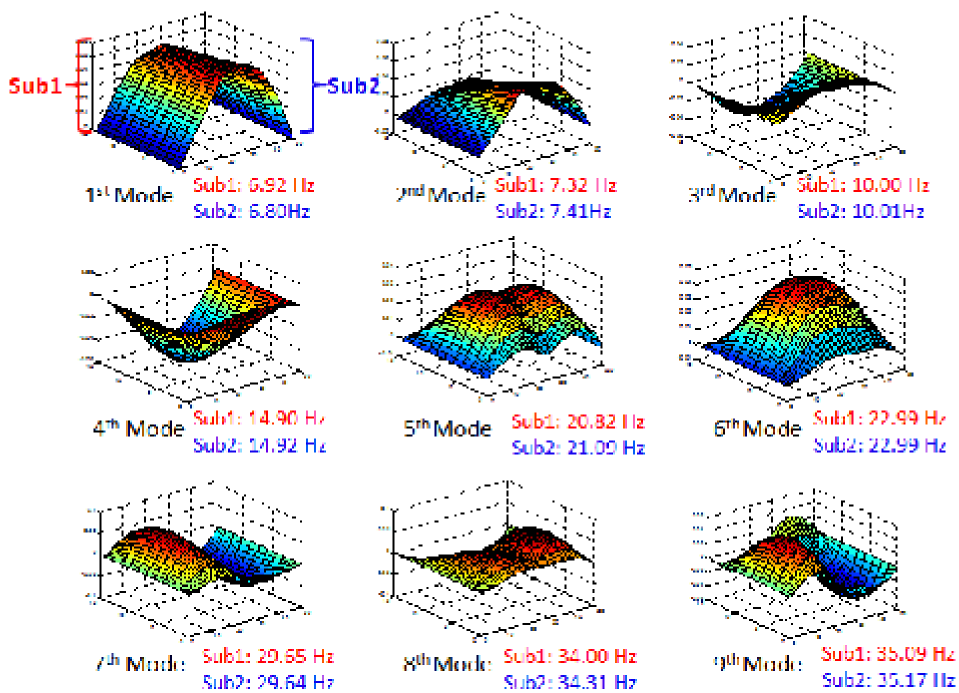

Figure 12. Mode shapes integrated by the two substructures

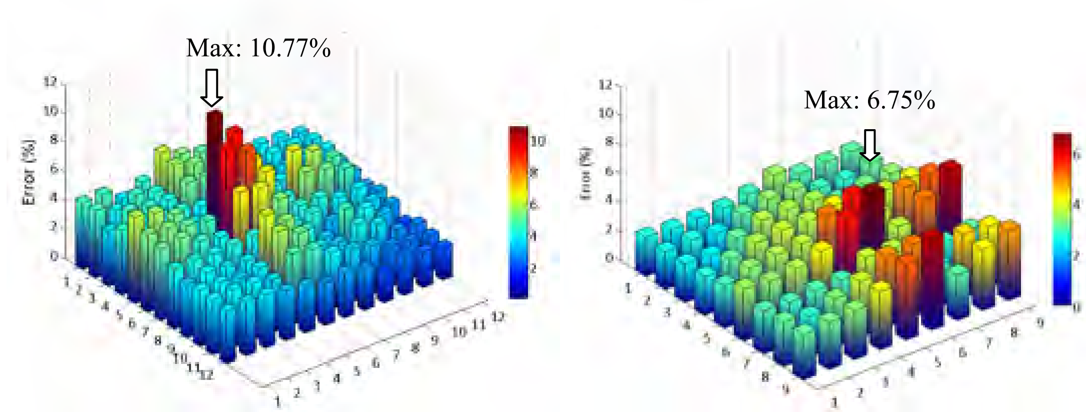

Figure 13. Error matrix of the integrated modal flexibility (a) Substructure 1 (b) Substructure 2

In order to validate the reliability of the substructure integration method, the original substructure flexibility is compared with the sub matrix in the resulting integrated global modal flexibility matrix. The relative error of each modal flexibility coefficient is compiled in the error matrices shown in Figure 13, where the maximum errors in two cases are 10.77% and 6.75%, and the average error for substructure 1 and 2 are 4.34% and 3.64%, respectively. The errors may be caused by the influence of traffic and other sources of noise and uncertainty common in experiments conducted on real structures. The relatively small errors prove the substructure integration method is reliable in cases where the uncertainties present are minimized.

6. CONCLUDING REMARKS

The concept of a rapid single input-multiple output (SIMO) impact testing device that will be capable of capturing modal parameters and estimating flexibility/deflection basins of common highway bridges during routine inspections is presented. The possibility of utilizing such a device for substructure testing and further integration has been verified by a numerical experiment and a real bridge test. It is shown that if properly designed and executed, the localized substructure tests may be used to estimate a complete flexibility matrix, which provides a sound basis for the envisioned rapid and quantitative condition assessment of bridges.

ACKNOWLEGEMENT

The authors express their deep appreciation to the Burlington County Bridge Commission and Pennoni Associates Inc. for their support.

REFERENCES

[1] ASCE "2005 Report Card for America's Infrastructure," http://www.asce.org/reportcard/2005/index2005.com

[2] ASCE "2009 Report Card for America's Infrastructure," http:// www.infrastructurereportcard.org

[3] FHWA, "National Bridge Inventory," U.S. Department of Transportation, Federal Highway Administration, Washington D.C., (2011).

[4] ASCE. Report card on America's infrastructure. www.asce.org/reportcard/2005, (2005).

[5] Aktan, A.E., Catbas, N., Turer, A. and Zhang, Z.F., "Structural identification: Analytical aspects," Journal of Structural Engineering. Papers 124(7), 817-829 (1998).

[6] Hogue, A.D., Aktan, A.E., and Hoyos, A., "Localized identification of constructed facilities," Journal of Structural Engineering. Papers 117(1), 128-148 (1991).

[7] Raghavendrachar, M., and Aktan, A.E., "Flexibility by multireference impact testing for bridge diagnostics," Journal of Structural Engineering. Papers 118(8), 2186-2203(1992).

[8] Catbas, F.N., Brown,D.L. and Aktan,A.E., "Use of modal flexibility for damage detection and condition assessments: Case studies and demonstrations on large structures," Journal of Structural Engineering, Papers 132(11): 1699-1712 (2006).

[9] Clough, Penzien. Dynamics of Structure. 1975

[10] Allemang, R.J., and Brown, D.L., "A unified polynomial approach to modal identification," Journal of Sound and Vibration, Papers 211(3), 301-322 (1998)

[11] Allemang, R.J."Vibrations: Experimental Modal Analysis," UC-Structural Dynamics Research Lab Publication, UC-SDRL-CN-20-263-663/664 (1995)